

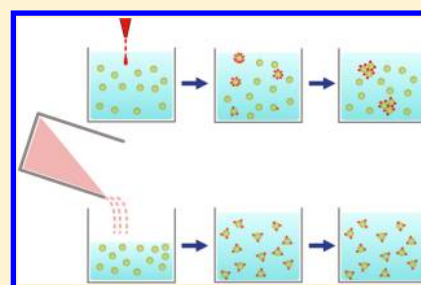
# Competition between Molecular Adsorption and Diffusion: Dramatic Consequences for SERS in Colloidal Solutions

Brendan L. Darby\* and Eric C. Le Ru\*

The MacDiarmid Institute for Advanced Materials and Nanotechnology School of Chemical and Physical Sciences, Victoria University of Wellington, P.O. Box 600, Wellington 6140, New Zealand

**S** Supporting Information

**ABSTRACT:** This study highlights a crucial but often overlooked consideration during sample preparation involving surface-adsorbing species: the competition between analyte adsorption and analyte diffusion/mixing strongly affects the distribution of analytes throughout the sample. In cases of fast analyte adsorption, we argue that the use of large-dilution factors, a common approach for sample preparation in surface-enhanced Raman spectroscopy (SERS), may result in an extreme nonuniformity of the surface coverage. This has a direct effect on the aggregation state of the colloidal solution and therefore on the overall SERS signal. Explicitly, we show that the average SERS signal obtained from typical dyes in colloidal solutions can be drastically different for two seemingly equivalent samples, differing only in the method by which the dye molecules were diluted. We, in addition, discuss the implications of such nonuniformity on the statistics of SERS intensities in the context of single-molecule detection. These results vividly highlight the importance of the dilution step in any experiments involving surface-adsorbing species and position SERS as an ideal tool to evidence such effects. In such cases, a simple half–half dilution procedure should be adopted as the standard method to mitigate these effects.



## INTRODUCTION

Dilutions form an essential part of most sample preparations in chemistry and biochemistry. Final concentrations may be affected by pipetting errors or by analyte adsorption onto walls, which can be important in the low-concentration regime or in microfluidic devices.<sup>1</sup> But once these issues are under control, it is generally assumed that the exact dilution procedure and in particular the chosen dilution factor have no influence on the prepared sample, providing final concentrations are the same. We here challenge this view in cases involving fast adsorption of the analyte onto the surface of nanoparticles. If such adsorption occurs faster than diffusion or mixing of the analyte across the solution, then one can intuitively expect that the distribution of analytes, notably the number of analytes per nanoparticle (coverage), will be strongly dependent on the dilution factor, and highly nonuniform in cases of large-dilution factors. Although the relevance of this effect should be assessed on a case-by-case basis, it in principle applies to a variety of chemical and biochemical systems relying on adsorption on nanoparticles, for example: studies of surface-functionalization of nanoparticles,<sup>2,3</sup> such as dye-sensitized quantum dots;<sup>4</sup> studies of biosensors based on immobilization of proteins onto nanoparticles;<sup>5</sup> any studies of the adsorption process itself, notably measurements of the adsorption isotherm and maximum coverage; and surface-enhanced spectroscopies<sup>6</sup> using metallic nanoparticle (NP) solutions. In fact, surface-enhanced Raman spectroscopy (SERS),<sup>7,8</sup> with its large sensitivity to adsorbed species and to NP aggregation, provides an ideal tool to further study this effect as will be shown.

Conversely, the realization of the importance of this effect for sample preparation may go some way toward improving the reproducibility of SERS in colloidal solutions.

For almost 30 years now, SERS has been poised to revolutionize analytical chemistry. Yet, despite intense research efforts, SERS is still viewed by most outside its research community as a technique plagued with problems: contradictory claims (for example, in terms of the SERS enhancement factors (EFs)),<sup>9</sup> unresolved questions (illustrated, for example, by the debate between electromagnetic and chemical enhancements), uncontrolled large signal fluctuations, and irreproducibility.<sup>10</sup> The first two items in this list are perhaps intrinsic to any research endeavor, but the latter two are particular weaknesses for a technique that should be more than mature enough to be an essential part of the analytical chemists toolbox.

Procedures have been developed to avoid signal fluctuations and improve reproducibility, at least in specific contexts. Efforts in this direction include more controlled SERS substrates,<sup>11–14</sup> rigorous definitions and quantification of the SERS EFs,<sup>15</sup> and promising quantification/calibration studies,<sup>16–20</sup> notably using internal standards.<sup>21</sup> The cause of the SERS fluctuations has also been better identified recently thanks to progress in single molecule SERS detection<sup>22,23</sup> and studies of the enhancement factor distribution<sup>24,25</sup> and the closely related concept of hot-

Received: April 17, 2014

Revised: June 25, 2014

Published: July 21, 2014

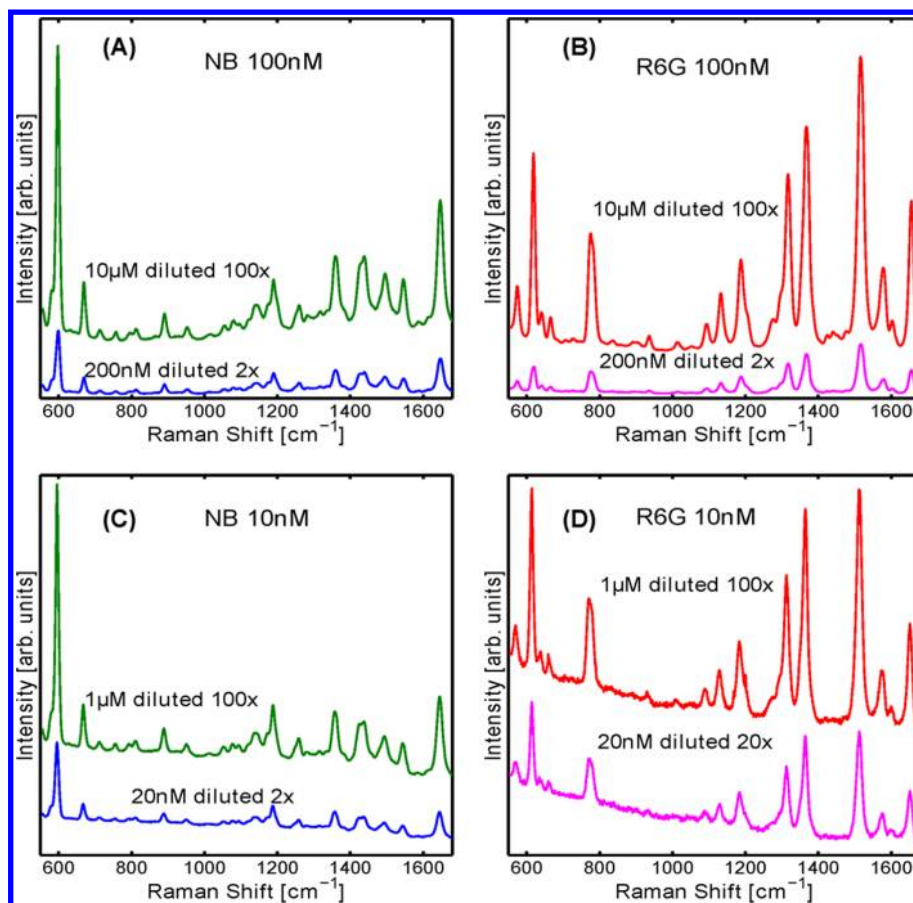


**Figure 1.** (A) Average SERS spectra in Ag colloid solution with 1 mM KCl, 100 nM Nile Blue (NB) prepared by diluting either a 10  $\mu\text{M}$  solution 100 times or a 200 nM solution two times. (B) Same for Rhodamine 6G (R6G). (C and D) Same as (A and B) with all concentrations reduced by a factor of 10.

spot,<sup>26</sup> which are highly localized regions (a few nm) where the SERS EF is extremely large.<sup>27</sup> The recognition of the presence of such hot-spots goes a long way in explaining the origin of the fluctuation/reproducibility problem,<sup>24,28</sup> especially in view of the fact that hot-spot properties are extremely sensitive to minute variations in the underlying geometry (for example subnanometer changes in the gap between two metallic NPs<sup>29</sup>). Recent and ongoing studies will no doubt improve dramatically our ability to seriously address the SERS fluctuation/reproducibility issue, both for general analytical chemistry applications and for single-molecule or trace detection studies. In this context, it is crucially important to identify additional potential sources of fluctuation/irreproducibility in SERS experiments.

We here highlight one such source of irreproducibility, namely, the dilution step in the important case of SERS in colloidal solutions, and demonstrate experimentally its dramatic impact for both average measurements and single molecule detection. By comparing large dilution factors and half–half dilutions, we show explicitly how two seemingly equivalent methods of sample preparation can result in markedly different SERS signals, by an order of magnitude in some cases. We argue that the observed discrepancy is very general, and can be explained by the competition between two kinetic processes: molecular adsorption on the metallic NPs and molecular diffusion and/or mixing into the rest of the solution. The importance of this effect is then further discussed in the context of single molecule SERS (SM-SERS) experiments.

This study vividly emphasizes the need to specify the method by which samples have been prepared, in particular all dilution steps. Moreover, we provide a simple strategy based on half–half-dilutions for ensuring the above sources of irreproducibility are avoided, and suggest that this method should be adopted as standard for sample preparation of colloidal solutions for SERS.

## ■ EXPERIMENTAL METHODS

**Sample Preparation.** For average SERS Enhancement Factor (Figure 5) and adsorption dynamics (Figure 3) measurements, Rhodamine 6G (R6G) and Nile Blue A (NB) were used as purchased from Sigma-Aldrich to prepare 100  $\mu\text{M}$  R6G and 10  $\mu\text{M}$  NB stock solutions in ultrapure water. Note that the solubility of NB in water is limited, hence, the lower concentration of the stock solution.<sup>30</sup> For the bianalyte SM-SERS experiments, a methyl ester version of Rhodamine 6G (3,6-bis(ethylamino)-9-[2-(methoxycarbonyl)phenyl]-xanthylum, referred to as R6M) and its partially deuterated version (d-R6M) were prepared in accordance with ref 31. Ag colloids were synthesized by the Lee and Meisel method.<sup>32</sup> A volume of Ag colloids was mixed with the required amount of KCl (2 mM for 1 mM and 20 mM for 10 mM final KCl concentration) in a half–half fashion and left to sit for 1 h. For the half–half dilution (HHD) method, 500  $\mu\text{L}$  of this solution was then mixed with 500  $\mu\text{L}$  of dye and again left for 1 h before measuring to allow all dye molecules to adsorb onto the surface of the NPs. For the large-dilution factor (LDF) method, 500  $\mu\text{L}$  of the colloid + KCl solution is first mixed with 490  $\mu\text{L}$  of water, and we then inject 10  $\mu\text{L}$  of dye solution of the appropriate concentration. All dilutions in this work are carried out with an autopipette by smoothly injecting the appropriate volume of dye solution into the prepared colloid solution contained in an ependorf tube. The injection step lasts

no more than 1 s. In each dilution step of the dye, from the stock solution down to the target SERS concentration, autopipettes are flushed three times with the parent dye solution before injecting into the final solution of water or colloids. This reduces wall adsorption of dye molecules and ensures that reproducible concentrations are achieved.

**Raman Measurements.** Raman measurements were carried out at 633 nm excitation in the backscattering configuration using a Jobin Yvon LabRam spectrometer equipped with a notch filter, a 600 l/mm grating, and a liquid-nitrogen cooled CCD detector. Laser power was set between 0.05 and 0.5 mW to maximize signal while avoiding any influence of dye photobleaching (notably for NB, which is excited close to resonance). For all average SERS measurements, spectra were acquired with a  $\times 20$  NA = 0.5 immersion objective (spot size  $\sim 5 \mu\text{m}$ , scattering volume of  $\sim 2000 \mu\text{m}^3$ ) integrating over 100 s to ensure averaging over many colloidal particles. Analytical SERS EFs were calculated as follows:<sup>15</sup> the effective SERS cross section of the 612  $\text{cm}^{-1}$  mode of R6G is estimated by comparison to the signal of a Raman standard under the same experimental conditions and then normalized to the measured<sup>15</sup> non-SERS cross-section at 633 nm of  $6.7 \times 10^{-28} \text{ cm}^2/\text{sr}$ . For SM-SERS measurements, spectra were acquired with a  $\times 100$  NA = 1.0 water-immersion objective (spot size  $\sim 1.2 \mu\text{m}$ , scattering volume of  $\sim 13 \mu\text{m}^3$ ), consecutively with each 0.1 s integration time. Average spectra for the nonmixed analytes, R6M and d-R6M, were also measured to facilitate the analysis. Each individual spectrum is then fitted within the spectral region of interest (550–700  $\text{cm}^{-1}$ ) as a superposition of these two reference spectra and a linear background using a linear least-square fit. The respective intensities of R6M and d-R6M for each spectrum is simply deduced from those fit and expressed as an equivalent SM-SERS EF (meaning the SM-SERS EF assuming only one molecule contributes to the signal). These are calculated as in ref 15, using the bare Raman cross sections for R6M and d-R6M as measured in ref 31. Further details about the SERS EF calculations are provided in the Supporting Information.

## RESULTS AND DISCUSSION

**Dilution Effects on Average SERS Signals.** Colloidal solutions arguably provide the simplest approach to preparing active SERS samples that produce the large enhancements required for ultralow concentration and single molecule detection. A standard colloidal SERS sample is prepared by simply adding the analyte to a solution of metal nanoparticles such that the analyte is diluted to the desired concentration for detection (concentrations of interest typically range from 1 pM to 100 nM). Although single NPs have recently been shown to be capable of single-molecule detection,<sup>28,33</sup> it is common practice to also induce partial aggregation of the NPs by means of the addition of aggregating agents such as KCl to redshift the resonance (toward the visible for silver NPs) and create gap regions of high enhancement, thereby boosting the SERS signal.<sup>26</sup> Such a method for preparation of SERS active colloidal solutions is well established and, except perhaps at ultralow concentrations where wall adsorption<sup>34</sup> may play a role, it is generally assumed that, providing standard basic rules are followed, the exact procedure for preparing a solution for a SERS measurement is irrelevant as long as the final concentrations (i.e., of metallic NPs, SERS probe, aggregating agents) are the same. In fact, most papers in the SERS literature do not specifically state if a 10 nM concentration of SERS probe was obtained by diluting 10 $\times$  from 100 nM, or 100 $\times$  from 1  $\mu\text{M}$ .

Figure 1 demonstrates that such an assumption is clearly wrong, at least in certain contexts. It illustrates the effect of the analyte dilution procedure on SERS intensity for two common SERS dyes, Nile Blue A (NB) and Rhodamine 6G (R6G), diluted in Lee and Meisel Ag colloids<sup>32</sup> premixed in 1 mM KCl.

At such a low concentration, KCl does not induce aggregation but is here used to remove the citrate layer on the NPs (which is replaced by Chlorine ions<sup>35,36</sup>) and thereby facilitate dye adsorption. We compare in Figure 1A the average SERS spectra from two 100 nM samples of NB prepared from a starting concentration of either 10  $\mu\text{M}$  diluted 100 $\times$  or 200 nM diluted 2 $\times$ . The intensity of the former is more than 4.5 times larger than that of the latter, despite the fact that all final concentrations (colloid, KCl, and dye) are nominally identical for both samples as can be seen from the detailed preparation procedure reproduced below:

- Sample 1: [[250  $\mu\text{L}$  Ag colloid + 250  $\mu\text{L}$  2 mM KCl] + 490  $\mu\text{L}$  H<sub>2</sub>O] + 10  $\mu\text{L}$  10  $\mu\text{M}$  NB.
- Sample 2: [250  $\mu\text{L}$  Ag colloid + 250  $\mu\text{L}$  2 mM KCl] + 500  $\mu\text{L}$  200 nM NB.

Similar results are obtained for R6G (Figure 1B), where the effect of dilution is even more pronounced with a factor of more than 7 between the two samples. Interestingly, the effect of sample dilution is less pronounced when the starting concentration of analyte is decreased as shown in Figure 1C,D, where all starting (and therefore final) concentrations of dyes were decreased by a factor of 10. Here the increase in intensity between equivalent 100 $\times$  and 2 $\times$  dilution samples is only a factor of about  $\sim 3$  for NB and  $\sim 2$  for R6G.

**Proposed Interpretation and Validation.** Our proposed explanation for these observations is based on the intuitive assumption that the kinetic for dye adsorption on the NPs is much faster than typical molecular diffusion times in the solution. Many SERS dyes (including R6G and NB) are cationic dyes to ensure strong adsorption onto the negatively charged metallic colloids through electrostatic interaction. Such a strong interaction is expected to result in very fast (subsecond) adsorption, at least in the early stages (low dye coverage) where steric hindrance does not play a role. In contrast, dye diffusion through a typical solution of 1 mL occurs on time scales of minutes or more. Indeed, typical diffusion coefficients for dyes are of the order of  $D = 10^{-5} \text{ cm}^2/\text{s}$  and correspond to a diffusion time through a distance  $L = 1 \text{ mm}$  of the order of  $\tau = L^2/D = 1000 \text{ s}$ . This is easily observed by injecting a small volume of high-concentration dye into a container of water and observing by eye the colored dye very slowly diffusing throughout the entire volume. In fact, diffusion-driven mixing is so slow that in most situations, convection effects will dominate and speed up the process; these include the unavoidable mechanical disturbance of injecting one solution in the other, and also possibly deliberate shaking/mixing. Even then, shaking or stirring can be expected to decrease the mixing time to a few seconds at best and should remain much slower than adsorption. If that is the case, then the majority of analytes are adsorbed before any diffusion/mixing occurs, i.e. in effect, they are adsorbed before being diluted to their final concentration. This then results in very different outcomes, depending on the starting concentration (or equivalently on the dilution factor).

Figure 2 schematically illustrates this effect. Figure 2A–C depicts the adsorption/mixing process in the case of large dilution factors (LDF), which seems to be the most commonly used method for preparing colloidal SERS samples. The final dye concentration is achieved by (Figure 2A) diluting a small volume of dye (for example 10  $\mu\text{L}$  of 10  $\mu\text{M}$ ) in a large volume of colloids (for example 990  $\mu\text{L}$  corresponding to a colloid to dye volume ratio of 99:1). Before mixing, the dye molecules are

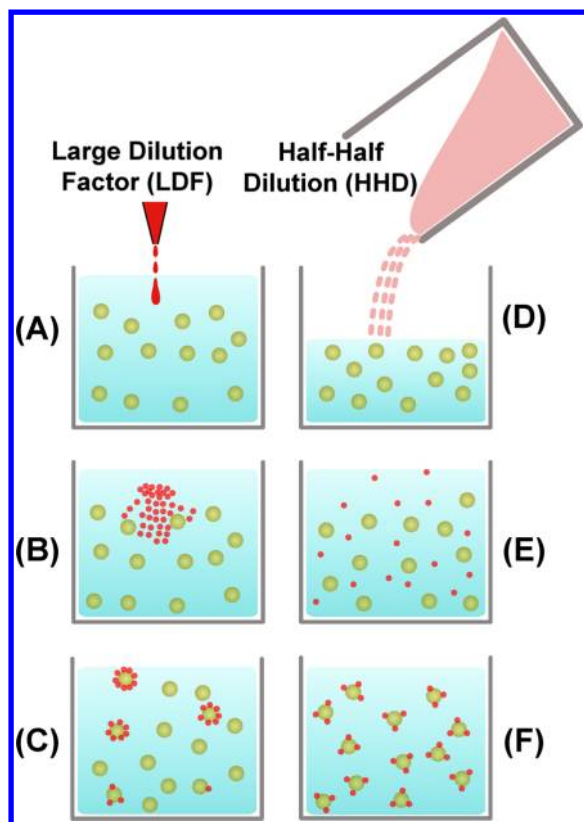


**Figure 2.** Schematic showing how two different dilution methods may lead to drastically different distributions of molecular coverage (number of analytes per colloid). The large dilution factor (LDF) method shown on the left (A–C) is typical of the majority of reported SERS experiments, while the half–half dilution (HHD) method shown on the right (D–F) is the method recommended in this work to obtain uniform molecular coverage.

at a much higher local concentration ( $10 \mu\text{M}$ ) in the small region they were injected into the sample (Figure 2B). Because adsorption occurs before diffusion/mixing, this results in a highly nonuniform distribution of the analytes on the NPs (Figure 2C), where only a small proportion of the NPs capture a large number of molecules (potentially 1% of the NPs have a molecular coverage 100 times larger than the expected average). This effect can be mitigated to a large extent by employing small dilution factors, ideally half–half dilutions (HHD), as shown in Figure 2D–F. The same final dye concentration (100 nM) is achieved by mixing equal volumes of dye ( $500 \mu\text{L}$  of 200 nM) and colloids ( $500 \mu\text{L}$ ) as shown in (Figure 2D). Convection-driven diffusion during mixing of the two volumes ensures in a first approximation that the dyes are dispersed throughout the sample uniformly (Figure 2E) and each dye molecule then adsorbs to the surface of the colloids through electrostatic interaction producing uniform molecular coverage throughout the sample (Figure 2F).

To support this hypothesis, we shall first demonstrate experimentally that molecular adsorption in the present system does occur on time scales faster than typical mixing times of a small volume into a larger one (which are of the order of seconds or larger). For this, we exploit the fact that the fluorescence signal of NB is quenched upon adsorption onto the metallic NPs. Any decrease in the fluorescence intensity when compared with a water solution of same concentration then clearly indicates that adsorption has started to occur. As

shown in Figure 3, strong fluorescence quenching is indeed observed in the first spectrum measured (i.e., within less than a

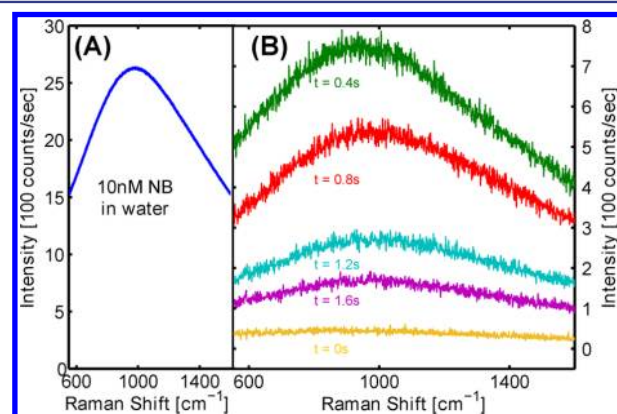


**Figure 3.** Dynamics of adsorption. (A) Reference fluorescence spectrum for 10 nM NB in water. (B) Fluorescence/Raman spectra of Ag colloids in 10 mM KCl to which we add (during measurement) an equal volume of 20 nM NB (to obtain 10 nM NB concentration). We show the five spectra obtained continuously (with a step of 0.4 s) at the time of mixing: one just before ( $t = 0$  s), and the first four just after. Even in the first spectrum right after addition of NB ( $t = 0.4$  s), the fluorescence is at most 1/3 of what it should be and reduces further to 1/10 after 1.2 s, indicating that a majority of NB molecules are adsorbed on a subsecond time scale. Also worthy to note is the appearance of the  $595 \text{ cm}^{-1}$  Raman peak of NB after 1.6 s. Note that the optical absorption by the colloid solution in this wavelength range is at most 10% and cannot explain the observed intensity drops.

second) following mixing of the dye and colloid solution. The adsorption process is therefore faster than can be resolved in such experiments (i.e., subsecond).

**Theoretical Support.** In reality the exact distribution of coverage obtained with the LDF method (Figure 2C) will depend on the details of the kinetics of adsorption vs mixing, and any intermediate situations between the extreme cases of Figure 2C,F can in principle be obtained. It is instructive to make this argument more quantitative by modeling the situation on a simple model system as shown in Figure 4. We consider a cylindrical container of radius 8 mm and height 2 cm (i.e., volume of 1 mL as for a typical sample preparation), into which the colloidal NPs are uniformly distributed and considered fixed since colloidal diffusion is much slower than dye/molecular diffusion. We then solve the diffusion equation (Fick's second law) for the analyte, coupled to a simple adsorption rate equation (which takes into account saturation at monolayer coverage), explicitly:

$$\frac{\partial c}{\partial t} = D \Delta c - k_A c \left( 1 - \frac{c}{c_{\text{sat}}} \right) \quad (1)$$

$$\frac{\partial c_A}{\partial t} = k_A c \left( 1 - \frac{c}{c_{\text{sat}}} \right) \quad (2)$$

$c(\mathbf{r}, t)$  and  $c_A(\mathbf{r}, t)$  represent the concentration of free and adsorbed analyte,  $D$  is the diffusion coefficient of the free analyte,  $k_A$  [ $\text{s}^{-1}$ ] characterizes the rate of adsorption at low coverage, and  $c_{\text{sat}}$  is the concentration at the saturation coverage (which we set at 500 nM here but note that this would depend on colloid concentration). The initial condition is set as  $c = c_0$  inside a small cylindrical volume of  $10 \mu\text{L}$  for the 100 $\times$  dilution (or 0.5 mL for a half–half dilution) and  $c = 0$  elsewhere (and  $c_A$

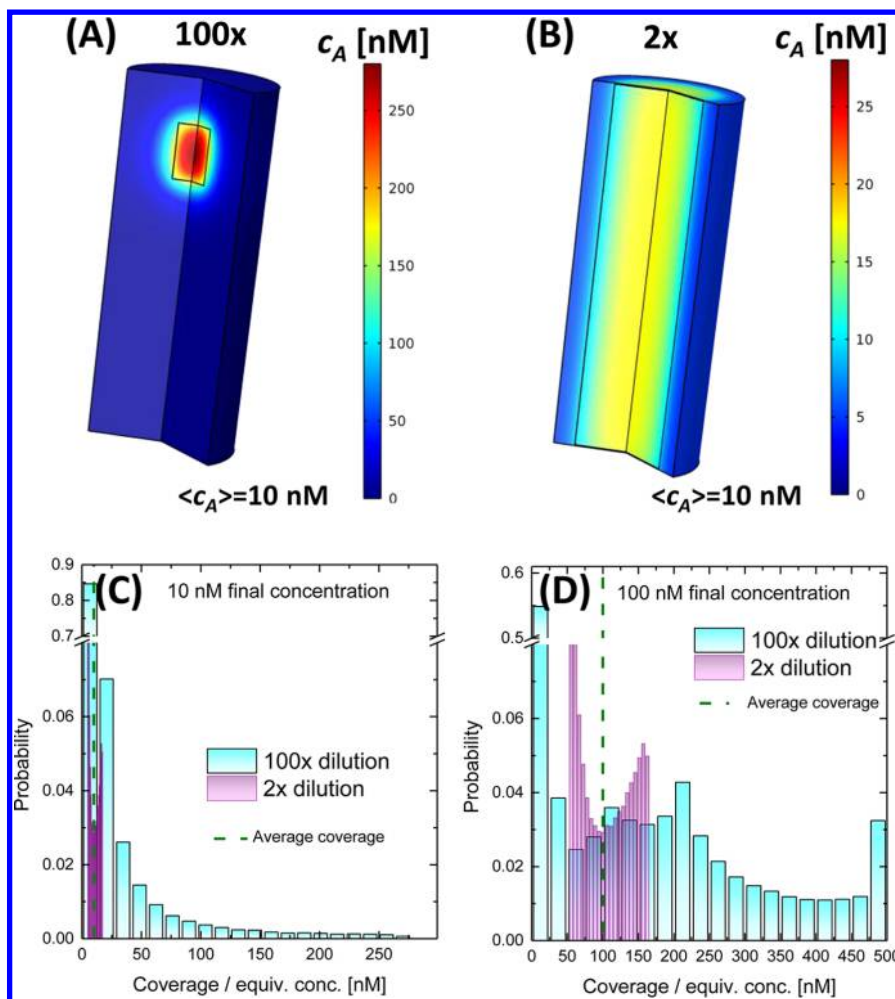


**Figure 4.** Theoretical predictions: the top panels show the geometry of the model and the map of the concentration of adsorbed molecules at long times for dilutions by (A) 100 $\times$  and (B) 2 $\times$  down to a final concentration of 10 nM. The corresponding distributions of molecular coverage in each case are shown in (C). The same predictions for a concentration 10 times larger, where saturation effects become more important, are shown in (D).

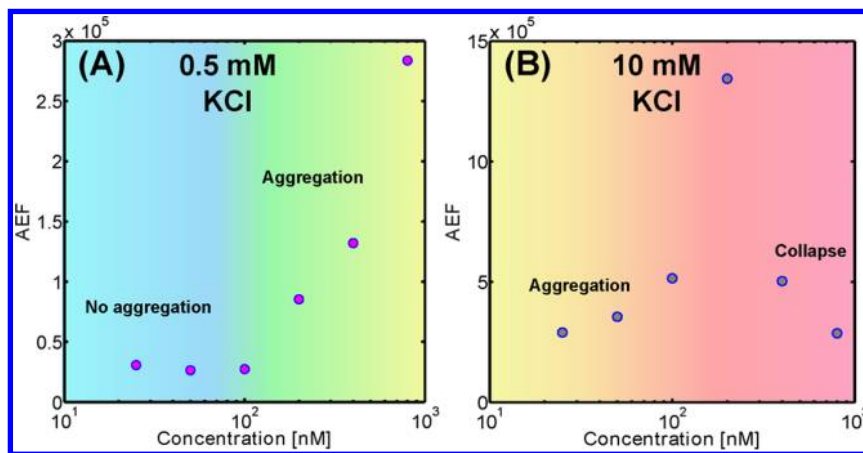


**Figure 5.** Measured average SERS EF at 633 nm excitation as a function of dye concentration for R6G in Ag colloid solution either (A) nonaggregated (in 0.5 mM KCl) or (B) preaggregated in 10 mM KCl.

= 0 everywhere). To model the convection-driven mixing/stirring, we set  $D$  at a value much larger than its normal free-diffusion estimates: we adjust it to  $D = 0.1 \text{ cm}^2/\text{s}$ , which results in a uniform concentration across the sample after about 10 s (in the absence of adsorption) and we set the adsorption rate  $k_A = 10 \text{ s}^{-1}$  (which here results in 95% adsorption in 0.3 s). The

problem is then solved with finite-element modeling in Comsol. From the long-time (typically 100 s) spatial distribution of the adsorbed species concentration  $c_A(\mathbf{r})$ , we can then compute the statistical properties of the distribution of adsorbed molecular coverage across the sample, i.e. average, maximum, and minimum coverages, or the histogram of

coverages. The results from these simulations are summarized in Figure 4. Surprisingly perhaps, even a half–half dilution results in a non-negligible spread of molecular coverage, but this would strongly depend on the exact details of the mixing procedure. For large dilution factors ( $100\times$ ), the predicted histograms of molecular coverage exhibit a much more spectacular nonuniformity, with maximum coverages as large as 25 times the average. At higher concentrations, a substantial proportion of NPs reach saturation coverage even if the target concentration is 5 times lower.

**Nanoparticle Aggregation.** In itself, the strong nonuniformity in molecular coverage as predicted in Figure 4 and illustrated in Figure 2F should not result in any difference in the average SERS signal, unless the SERS EF depends nonlinearly on the molecular coverage. In colloidal SERS solution, there is an obvious mechanism providing such a nonlinear dependence: dye-induced colloid aggregation.<sup>37</sup> It is well established that aggregated colloidal solutions exhibit much larger SERS EF<sup>14,26,35,36,38,39</sup> (up to a point where overaggregation results in complete collapse/sedimentation of the colloidal solution). Aggregation is typically induced by the addition of electrolyte, which screens the electrostatic repulsion between the negatively charged colloids. Aggregation can also be induced by adsorption of positively charged analytes<sup>35,36,40</sup> (like NB and R6G) as this will reduce the net negative charge of the NPs. As the molecular coverage increases, the net charge is further reduced and the aggregation is further favored. One therefore expects an increase in average SERS EF as a function of molecular coverage as a result of analyte-induced aggregation.

This phenomenon is evidenced experimentally in Figure 5. The average SERS EF of R6G adsorbed to silver nanoparticles is measured as a function of dye concentration in two regimes; in (A) dyes are added to colloids in 0.5 mM KCl (so as to replace the surface citrate layer but not cause aggregation of colloids) and in (B) dyes are added to colloids in 10 mM KCl (so as to preaggregate the colloids, as most SERS studies are performed). Previous studies<sup>41</sup> have shown this to be the optimal concentration of KCl for producing large SERS EFs with Lee and Meisel colloids. All samples were prepared by using the half–half dilution method to ensure uniform surface coverage of colloids, whose final concentration is 1/4 of the as-synthesized solution. For unaggregated colloids (Figure 5A), the EF for dye concentrations of 25, 50, and 100 nM are essentially equal; in other words, the SERS intensity scales linearly with concentration. However, above 100 nM (which we here estimate to correspond to about 6000 dyes per particle), the EF increases significantly from about  $3\times 10^4$  up to  $3\times 10^5$ , an increase that can be attributed to dye-induced colloid aggregation. For preaggregated colloids (Figure 5B), the effect of KCl-induced aggregation is clearly evident in the order of magnitude difference (10 times larger) in SERS EF at the lowest concentration (25 nM). Moreover, because the colloids are already partially aggregated, even a small concentration of positively charged analyte further induces aggregation of the colloid, and this is reflected in the concomitant increase in SERS EF from the lowest dye concentrations (from 25 nM to 50 nM and 100 nM). The measured EF keeps increasing up to a maximum of  $1.3\times 10^6$  at 200 nM, beyond which the colloidal solution collapses/sediments resulting in a sharp drop in SERS signal. It should be noted that partially aggregated Lee and Meisel colloids do not exhibit any well-defined aggregate extinction peak and extinction spectra cannot here be used as a proxy for the aggregation state.<sup>42</sup>

These results clearly highlight the effect of molecular coverage on colloid aggregation in our system, and can now be linked to the observed dilution effects. When large dilution factors are used, the strongly nonuniform coverage may result in aggregation for the small number of colloids with the highest coverage, and therefore in a larger SERS EF for those colloids. Since the aggregated colloids are those with the most dyes, the average SERS EF for the entire solution is also increased. For example, from Figure 5A, we see that a 100 nM solution with uniform coverage (i.e., prepared from the HHD method) exhibits an average enhancement of  $10^4$ . The same solution prepared using a  $100\times$  dilution (from 10  $\mu$ M) will contain many NPs with no adsorbate and many NPs with coverage close to saturation (see Figure 4D). The higher local concentration will clearly cause local aggregation of the minority of colloids in the region where the dye is injected, and the EF for these will be of the order of  $10^5$  (according to Figure 5A). The overall SERS signal will be increased by a factor up to 10, depending on the details of the competition between molecular adsorption and mixing dynamics. This explains the factors of 4.5 and 7 observed for NB and R6G in Figure 1A,B.

It is important to note that the LDF method could be affected by a number of factors that cannot be controlled accurately: how the low volume of dye is injected into the solution, whether mechanical stirring is applied, etc.. The increase in SERS EF from the LDF method to the HHD method could therefore be highly nonreproducible under nominally identical preparation conditions. It would also strongly depend on the actual dilution factor (as hinted at in Figures 1,4). These considerations clearly show that the high-concentration/low-volume dilution approach should always be avoided when preparing colloidal solutions. In fact, these issues can simply be eliminated by carrying out equal-volume mixing/dilution.

**Single Molecule Statistics.** While we have focused so far on average SERS EF, it is clear that the strong nonuniformity in molecular coverage resulting from large-factor dilutions should also have a profound effect on the statistics of SERS signals. This should particularly affect single-molecule SERS studies where coverage estimates and statistics of signals play a crucial role in identifying the correct conditions for single-molecule detection. We therefore now highlight the consequences of our findings for single molecule SERS (SM-SERS).

First, it is clear that the average molecular coverage has little meaning in the case of samples prepared by the LDF method, since a small number of NPs will have a much larger number of molecules. The original studies of SM-SERS<sup>43–45</sup> in fact relied on such estimates to justify the single molecule nature of the SERS signals. The targeted concentration was adjusted such that *on average*, less than one molecule (say 0.5) was measured at a given time. SERS events were then rare occurrences, but they were attributed to SM-SERS. It is now clear from this study that if the samples are prepared using a  $100\times$  dye-dilution, then a small fraction of nanoparticles could in fact have a much larger coverage than average (0.5), with up to say 10 molecules per NPs. The rare SERS events would then most likely correspond to those high-coverage particles rather than to SM-SERS.

In fact, as discussed in ref 46, there were many additional potential problems with the low-concentration approach, which prompted the development of bianalyte SERS<sup>46</sup> as a more convincing and statistically robust method of studying SM-

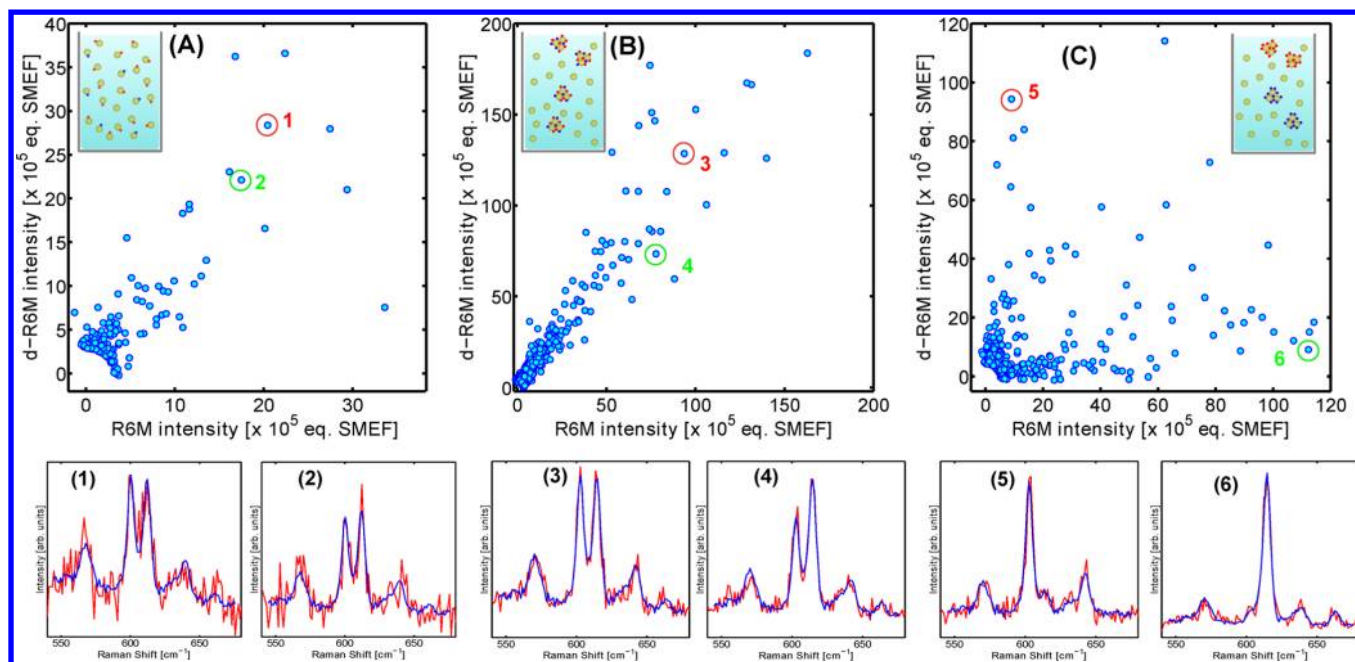


**Figure 6.** Effect of different sample dilution procedures on the statistics of bianalyte single molecule SERS spectra using isotopic partners R6M and d-R6M at 10 nM. Scatter plots of the intensity of the  $612\text{ cm}^{-1}$  peak of R6M ( $x$ -axis) and the  $600\text{ cm}^{-1}$  peak of d-R6M ( $y$ -axis) for (A) samples where dyes are premixed together and then diluted with the HHD method, (B) dyes are premixed together and then diluted using the LDF method with  $100\times$  dilution, and (C) dyes are added sequentially to the NP solution using the LDF method with  $100\times$  dilution. In each case, a schematic showing the expected outcome of the dilution is shown as an inset. In all cases, Ag colloid are premixed with 20 mM for preaggregation. Representative spectra (1–6) are shown at the bottom along with the corresponding fits to a mixture R6M and d-R6M spectra. Note that the intensity scales are different for each panel but can be read from the corresponding circles in the upper panels (A–C).

SERS.<sup>47,48</sup> Within this framework, two analytes with comparable SERS cross-section but a distinguishable SERS spectrum, are used to experimentally determine the nature of the SERS events, either predominantly SM-SERS or multimolecule SERS,<sup>28,49</sup> without any assumptions on the coverage. Ideal implementations of the method make use of two isotopically different versions of the same molecule.<sup>31,50,51</sup> Central to the interpretations of any bianalyte SERS experiment is the implicit assumption that the distribution of molecules across the sample is the same (even if potentially nonuniform) for both bianalyte partners. This aspect was implicit in the original bianalyte work,<sup>46,49</sup> and, in the light of the current study, needs to be clearly re-emphasized. We demonstrate explicitly in Figure 6 how the wrong conclusions about the SM-SERS regime could be attained because of the dilution problems evidenced in this work. Figure 6 shows a typical bianalyte SERS analysis, where we plot the SERS intensities of one dye vs the other (we here use a modified rhodamine 6G and its isotopically substituted partner with 4 deuterium atoms as studied in detail in<sup>31</sup>). In Figure 6A, most events are mixed, which correspond to the multimolecule regime, as expected for this system at this dye concentration (10 nM). In this first instance, both bianalyte partners were mixed together at  $1\ \mu\text{M}$ , then diluted to 20 nM, and then diluted by a factor of 2 with the final colloid solution, i.e. we use the HHD method recommended in this work to avoid dilution problem. However, in most previous works, it is likely that large dilution factors were used, and the results obtained from an equivalent  $100\times$  dilution are therefore shown in Figure 6B. As expected from the previous discussion, a small number of NPs exhibit much higher coverage (for both molecules) and this is reflected in the relatively larger events that are observed, and in the stronger concentration of events around the 50%–50% line,

indicating an even more pronounced multimolecule regime than obtained from Figure 6A. An even more spectacular consequence of the dilution problem is evidenced in Figure 6C, where the bianalyte partners were diluted  $100\times$  sequentially into the colloid solution, instead of being premixed together as in Figure 6A,B. In such a case, those NPs with a larger than average coverage of one dye are not the same as those for the other dye. The statistics of events then become characteristic of the single-molecule regime, with several pure events of one dye or the other. These seemingly SM-SERS events in reality correspond to NPs with a large coverage of one dye and not the other and in view of Figure 6A,B are *not* SM-SERS events. The dilution procedure therefore here introduces artifacts that lead to an entirely wrong conclusion regarding SM-SERS.

These observations clearly suggest that, in the context of SM-SERS, only bianalyte experiments where dyes are premixed before dilution into colloids can be trusted. It is difficult to assess whether such problems have affected previous studies, since such preparation details are not always specified.<sup>52</sup> Figure 6 focuses on demonstrating the risk of erroneous claims of SM-SERS detection if the bianalyte partners are not premixed together and the LDF method is used. From the results of this study, it should also be clear that even if the bianalyte partners are premixed, the HHD method should be strongly preferred to avoid nonuniform coverage across the sample and irreproducibility. Indeed, large variations in surface coverage may result in part of the sample being in the single-molecule regime and part in the multimolecule regime, therefore blurring and confusing the statistical analysis on SM-SERS intensities. We therefore expect that the adoption of the HHD method for SM-SERS studies will result in much stronger conclusions and a much clearer transition between the single-molecule and

multimolecule regime. Further work is in progress in this direction.

## CONCLUSION

We have clearly demonstrated how apparently similar dilution/preparation methods of colloidal SERS solutions can result in drastically different properties, in terms of both average signals and their statistics in the context of single molecule detection. Large dilution factors of the analytes into the NPs solution create a large variation in molecular coverage per NPs across the sample. This effect is naturally interpreted as a consequence of the competition between the typically fast analyte adsorption onto NPs and the comparatively slow diffusion/mixing process, even when driven by forced convection (shaking/stirring). As such, this effect is not expected to be general, and will only affect experiments where the analyte adsorption is much faster than the mixing time. It is possible that noncationic analytes, which are less attracted to the negatively charged colloids, may not be affected by this problem because they adsorb more slowly, but this should be assessed on a case-by-case basis. Nevertheless, the examples presented in this study clearly show that this effect is indeed important for analytes (such as Rhodamine 6G and Nile Blue) and colloidal solutions (Lee and Meisel Ag colloids) that are commonly used and studied. It may therefore have had a dramatic (but unnoticed) impact on the interpretations of many previous SERS studies. We have shown in particular how certain sample preparation methods can lead to extreme misinterpretations of the nature of single molecule SERS spectra when using the bianalyte technique. Moreover, although we have here focused on the analyte dilution step only, we have observed similar problems when mixing the colloidal solution with salts such as KCl using large-dilution factors (for example 100 mM KCl diluted 10 $\times$ ). Similar interpretations as presented here apply in such a case and such preparation procedures should be avoided.

These findings highlight the necessity for authors to specify clearly the exact method by which samples were prepared, particularly in the case of colloidal solutions. Perhaps more importantly, most of these problems can be largely avoided by simply using low-dilution factors, i.e., the half/half dilution method, which we therefore recommend as the golden standard for any SERS experiments involving colloidal solutions. We believe our results provide crucial insight into a simple but often overlooked aspect of SERS experiments and shed light on yet another common source of error in the SERS literature. The conclusions of this work would also extend naturally to dilutions in any chemical systems where a fast local phenomenon such as adsorption may compete with the diffusion/mixing process and may therefore have implications well beyond SERS.

## ASSOCIATED CONTENT

### Supporting Information

Details of enhancement factor determinations and additional figure showing the data of Figure 5 plotted as SERS intensities as a function of concentration. This material is available free of charge via the Internet at <http://pubs.acs.org>.

## AUTHOR INFORMATION

### Corresponding Authors

brendan.darby2@gmail.com  
eric.leru@vuw.ac.nz

## Notes

The authors declare no competing financial interest.

## ACKNOWLEDGMENTS

The authors thank Chris Galloway for insightful feedback on the manuscript. E.C.L.R. thanks the Royal Society of New Zealand (RSNZ) for support through a Marsden Grant and Rutherford Discovery Fellowship.

## REFERENCES

- (1) Koc, Y.; de Mello, A. J.; McHale, G.; Newton, M. I.; Roach, P.; Shirtcliffe, N. J. *Lab Chip* **2008**, *8*, 582–586.
- (2) Erathodiyil, N.; Ying, J. Y. *Acc. Chem. Res.* **2011**, *44*, 925–935.
- (3) Jiang, S.; Win, K. Y.; Liu, S.; Teng, C. P.; Zheng, Y.; Han, M.-Y. *Nanoscale* **2013**, *5*, 3127–3148.
- (4) Walker, B. J.; Nair, G. P.; Marshall, L. F.; Bulovic, V.; Bawendi, M. G. *J. Am. Chem. Soc.* **2009**, *131*, 9624–9625.
- (5) Roach, P.; Farrar, D.; Perry, C. C. *J. Am. Chem. Soc.* **2006**, *128*, 3939–3945.
- (6) Aroca, R. F. *Surface-Enhanced Vibrational Spectroscopy*; John Wiley & Sons: Chichester, 2006.
- (7) Moskovits, M. *Rev. Mod. Phys.* **1985**, *57*, 783–826.
- (8) Le Ru, E. C.; Etchegoin, P. G. *Principles of Surface Enhanced Raman Spectroscopy and Related Plasmonic Effects*; Elsevier: Amsterdam, 2009.
- (9) Le Ru, E. C.; Etchegoin, P. G. *MRS Bull.* **2013**, *38*, 631–640.
- (10) Natan, M. J. *Faraday Discuss.* **2006**, *132*, 321–328.
- (11) Braun, G.; Pavel, I.; Morrill, A. R.; Seferos, D. S.; Bazan, G. C.; Reich, N. O.; Moskovits, M. *J. Am. Chem. Soc.* **2007**, *129*, 7760–7761.
- (12) Roca, M.; Haes, A. J. *J. Am. Chem. Soc.* **2008**, *130*, 14273–14279.
- (13) Zhang, X.; Zhao, J.; Whitney, A. V.; Elam, J. W.; Van Duyne, R. P. *J. Am. Chem. Soc.* **2006**, *128*, 10304–10309.
- (14) Taylor, R. W.; Lee, T.-C.; Scherman, O. A.; Esteban, R.; Aizpurua, J.; Huang, F. M.; Baumberg, J. J.; Mahajan, S. *ACS Nano* **2011**, *5*, 3878–3887.
- (15) Le Ru, E. C.; Blackie, E.; Meyer, M.; Etchegoin, P. G. *J. Phys. Chem. C* **2007**, *111*, 13794–13803.
- (16) Faulds, K.; Smith, W. E.; Graham, D. *Anal. Chem.* **2004**, *76*, 412–417.
- (17) Ackermann, K. R.; Henkel, T.; Popp, J. *ChemPhysChem* **2007**, *8*, 2665–2670.
- (18) Bell, S. E. J.; Sirimuthu, N. M. S. *Chem. Soc. Rev.* **2008**, *37*, 1012–1024.
- (19) Kasper, S.; Biedermann, F.; Baumberg, J. J.; Scherman, O. A.; Mahajan, S. *Nano Lett.* **2012**, *12*, 5924–5928.
- (20) Guerrini, L.; Pazos, E.; Penas, C.; Vázquez, M. E.; Mascareñas, J. L.; Alvarez-Puebla, R. A. *J. Am. Chem. Soc.* **2013**, *135*, 10314–10317.
- (21) Zhang, D.; Xie, Y.; Deb, S. K.; Davison, V. J.; Ben-Amotz, D. *Anal. Chem.* **2005**, *77*, 3563–3569.
- (22) Etchegoin, P. G.; Le Ru, E. C. *Phys. Chem. Chem. Phys.* **2008**, *10*, 6079–6089.
- (23) Pieczonka, N. P. W.; Aroca, R. F. *Chem. Soc. Rev.* **2008**, *37*, 946–954.
- (24) Le Ru, E. C.; Etchegoin, P. G.; Meyer, M. J. *Chem. Phys.* **2006**, *125*, 204701.
- (25) Fang, Y.; Seong, N.-H.; Dlott, D. D. *Science* **2008**, *321*, 388–391.
- (26) Jiang, J.; Bosnick, K.; Maillard, M.; Brus, L. *J. Phys. Chem. B* **2003**, *107*, 9964–9972.
- (27) Le Ru, E. C.; Etchegoin, P. G. *Annu. Rev. Phys. Chem.* **2012**, *63*, 65–87.
- (28) Le Ru, E. C.; Grand, J.; Sow, I.; Somerville, W. R. C.; Etchegoin, P. G.; Treguer-Delapierre, M.; Charron, G.; Felidj, N.; Levi, G.; Aubard, J. *Nano Lett.* **2011**, *11*, 5013.
- (29) Jain, P. K.; Huang, W.; El-Sayed, M. A. *Nano Lett.* **2007**, *7*, 2080–2088.

- (30) Reigue, A.; Auguie, B.; Etchegoin, P. G.; Le Ru, E. C. *J. Raman Spectrosc.* **2013**, *44*, 573–581.
- (31) Blackie, E.; Le Ru, E. C.; Meyer, M.; Timmer, M.; Burkett, B.; Northcote, P.; Etchegoin, P. G. *Phys. Chem. Chem. Phys.* **2008**, *10*, 4147–4153.
- (32) Lee, P. C.; Meisel, D. *J. Phys. Chem.* **1982**, *86*, 3391–3395.
- (33) Zrimsek, A. B.; Henry, A.-I.; Van Duyne, R. P. *J. Phys. Chem. Lett.* **2013**, *4*, 3206–3210.
- (34) Hildebrandt, P.; Stockburger, M. *J. Phys. Chem.* **1984**, *88*, 5935–5944.
- (35) Futamata, M.; Maruyama, Y. *Appl. Phys. B: Laser Opt.* **2008**, *93*, 117–130.
- (36) Futamata, M.; Yu, Y.; Yajima, T. *J. Phys. Chem. Soc.* **2011**, *115*, 5271–5279.
- (37) Pierre, M. C. S.; Mackie, P. M.; Roca, M.; Haes, A. J. *J. Phys. Chem. C* **2011**, *115*, 18511–18517.
- (38) Schwartzberg, A. M.; Grant, C. D.; Wolcott, A.; Talley, C. E.; Huser, T. R.; Bogomolni, R.; Zhang, J. Z. *J. Phys. Chem. B* **2004**, *108*, 19191–19197.
- (39) Shaw, C. P.; Fan, M.; Lane, C.; Barry, G.; Jirasek, A. I.; Brolo, A. G. *J. Phys. Chem. C* **2013**, *117*, 16596–16605.
- (40) Lebovka, N. I. *Adv. Polym. Sci.* **2014**, *255*, 57–96.
- (41) Meyer, M.; Le Ru, E. C.; Etchegoin, P. G. *J. Phys. Chem. B* **2006**, *110*, 6040–6047.
- (42) Le Ru, E. C.; Galloway, C.; Etchegoin, P. G. *Phys. Chem. Chem. Phys.* **2006**, *8*, 3083–3087.
- (43) Kneipp, K.; Wang, Y.; Kneipp, H.; Perelman, L. T.; Itzkan, I.; Dasari, R. R.; Feld, M. S. *Phys. Rev. Lett.* **1997**, *78*, 1667–1670.
- (44) Nie, S.; Emory, S. R. *Science* **1997**, *275*, 1102–1106.
- (45) Xu, H.; Bjerneld, E. J.; Käll, M.; Börjesson, L. *Phys. Rev. Lett.* **1999**, *83*, 4357–4360.
- (46) Le Ru, E. C.; Meyer, M.; Etchegoin, P. G. *J. Phys. Chem. B* **2006**, *110*, 1944–1948.
- (47) Goulet, P. J.; Aroca, R. F. *Anal. Chem.* **2007**, *79*, 2728–2734.
- (48) Titus, E. J.; Weber, M. L.; Stranahan, S. M.; Willets, K. A. *Nano Lett.* **2012**, *12*, 5103–5110.
- (49) Etchegoin, P. G.; Meyer, M.; Blackie, E.; Le Ru, E. C. *Anal. Chem.* **2007**, *79*, 8411–8515.
- (50) Dieringer, J. A.; Lettan, R. B., II; Scheidt, K. A.; Van Duyne, R. P. *J. Am. Chem. Soc.* **2007**, *129*, 16249–16256.
- (51) Kleinman, S. L.; Ringe, E.; Valley, N.; Wustholz, K. L.; Phillips, E.; Scheidt, K. A.; Schatz, G. C.; Van Duyne, R. P. *J. Am. Chem. Soc.* **2011**, *133*, 4115–4122.
- (52) Patra, P. P.; Kumar, G. V. P. *J. Phys. Chem. Lett.* **2013**, *4*, 1167–1171.

# Supporting information for “Competition between molecular adsorption and diffusion: dramatic consequences for SERS in colloidal solutions”

Brendan L. Darby\* and Eric C. Le Ru†

*The MacDiarmid Institute for Advanced Materials and Nanotechnology  
School of Chemical and Physical Sciences  
Victoria University of Wellington  
PO Box 600 Wellington, New Zealand*

## S.I. DETAILS OF ENHANCEMENT FACTOR CALCULATIONS

All SERS enhancement factors (EFs) quoted in Fig. 5 and 6 are determined following the methods of Ref. 1.

### A. Average SERS enhancements

The average SERS enhancements are calculated as analytical enhancement factors (AEF) as defined in Ref. 1:

$$\text{AEF} = \frac{I_{\text{SERS}}/c_{\text{SERS}}}{I_{\text{RS}}/c_{\text{RS}}}. \quad (\text{S1})$$

where  $I_{\text{SERS}}$  is the measured SERS intensity for a dye concentration  $c_{\text{SERS}}$  and  $I_{\text{RS}}$  is the normal Raman intensity of a solution of possibly different (typically higher) concentration  $c_{\text{RS}}$  under the same experimental conditions.

In practice, the latter can be characterized by the Raman cross-section [2] and has been measured to be  $d\sigma_{\text{RS}}/d\Omega = 6.7 \times 10^{-28} \text{ cm}^2/\text{sr}$  for the  $612 \text{ cm}^{-1}$  peak of Rhodamine 6G excited at  $633 \text{ nm}$  [1].

By comparing the SERS intensity to that of a known Raman standard, here 2-bromo-2-methylpropane (2B2MP), under the same experimental conditions, we can infer an effective SERS cross-sections as:

$$\frac{d\sigma_{\text{SERS}}^{\text{Ave}}}{d\Omega} = \frac{I_{\text{SERS}}/c_{\text{SERS}}}{I_{2\text{B2MP}}/c_{2\text{B2MP}}} \frac{d\sigma_{2\text{B2MP}}}{d\Omega}. \quad (\text{S2})$$

where the  $c_{2\text{B2MP}} = 8.8 \text{ M}$  is concentration of pure 2B2MP and  $d\sigma_{2\text{B2MP}}/d\Omega = 5.4 \times 10^{-30} \text{ cm}^2/\text{sr}$  is the reference Raman cross-section of the  $516 \text{ cm}^{-1}$  mode of 2B2MP at  $633 \text{ nm}$  [1].

The AEF is then obtained from

$$\text{AEF} = \frac{d\sigma_{\text{SERS}}^{\text{Ave}}/d\Omega}{d\sigma_{\text{RS}}/d\Omega}. \quad (\text{S3})$$

### B. Single-molecule enhancements

For average EF estimations, we do not need to know the actual number of measured molecules as only relative numbers appear in the calculation and they can therefore be calculated as the ratio of concentrations. This is no longer the case when estimating the SERS EF corresponding to a single-molecule event. To estimate the SERS cross-section of a single molecule, it needs to be compared to the Raman intensity of a single molecule of our Raman standard 2B2MP. Although this cannot be measured directly as it is too weak, it can be inferred from a careful characterization of the effective scattering volume  $V_{\text{eff}}$  as explained in Ref. 1. In the SM-SERS experiments reported here, the waist of the exciting beam at the focal point is  $w_0 \sim 0.63 \mu\text{m}$  and the effective height of the scattering volume (as defined in 1) is  $H_{\text{eff}} \sim 21 \mu\text{m}$ , and we therefore have  $V_{\text{eff}} \sim 13 \mu\text{m}^3$ . From this, we obtain the single-molecule SERS cross-section for a given SM-SERS event of intensity  $I_{\text{SERS}}^{\text{SM}}$  to be:

$$\frac{d\sigma_{\text{SERS}}^{\text{SM}}}{d\Omega} = \frac{I_{\text{SERS}}^{\text{SM}}}{I_{2\text{B2MP}}/(\mathcal{N}c_{2\text{B2MP}}V_{\text{eff}})}. \quad (\text{S4})$$

As for the AEF, the  $612 \text{ cm}^{-1}$  mode of Rhodamine 6G and the  $516 \text{ cm}^{-1}$  mode of 2B2MP are used for the calculations and the SMEF is then obtained as:

$$\text{SMEF} = \frac{d\sigma_{\text{SERS}}^{\text{SM}}/d\Omega}{d\sigma_{\text{RS}}/d\Omega}. \quad (\text{S5})$$

## S.II. DEPENDENCE OF SERS INTENSITIES ON CONCENTRATION

The data of Fig. 5 are plotted in Fig. S1 in terms of SERS intensities (instead of SERS EF as in the main text). In this format, these plots provide an indirect measurement of the adsorbate concentration in the region where no aggregation occurs.

\*Electronic address: [brendan.darby2@gmail.com](mailto:brendan.darby2@gmail.com)

†Electronic address: [eric.leru@vuw.ac.nz](mailto:eric.leru@vuw.ac.nz)

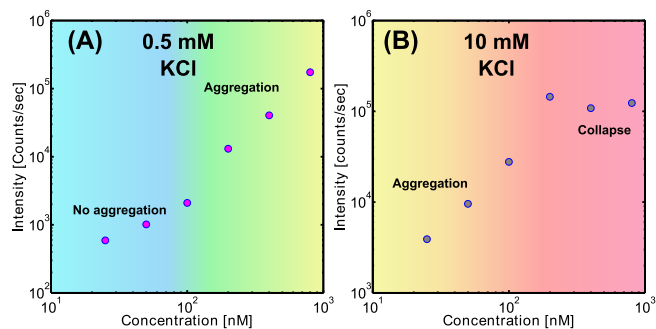


FIG. S1: Measured average SERS intensity at 633 nm excitation as a function of dye concentration for Rhodamine 6G in Ag colloid solution either (A) non-aggregated (in 0.5 mM KCl) or (B) pre-aggregated in 10 mM KCl. These are the same data as Fig. 5 of the manuscript. The “no-aggregation” region at low concentration reflects the linear dependence of surface adsorbates with dye concentration, as would be measured in an adsorption isotherm, but this correspondence fails once the colloidal solution start aggregating. Note also that the adsorption isotherm is an average property and would not in general reveal non-uniformity in the adsorbate concentration, as evidenced in this work.

- 
- [1] E. C. Le Ru, E. Blackie, M. Meyer, and P. G. Etchegoin, *J. Phys. Chem. C* **111**, 13794 (2007).  
 [2] E. C. Le Ru and P. G. Etchegoin, *Principles of Surface*

*Enhanced Raman Spectroscopy and Related Plasmonic Effects* (Elsevier, Amsterdam, 2009).